IBRACON Structures and Materials Journal
Revista IBRACON de Estruturas e Materiais
ISSN 1983-4195 ismj.org

ORIGINAL ARTICLE

Influence of exposure temperature variability on concrete degradation as a function of compressive strength and ultrasonic wave propagation velocity

Influência da variabilidade da temperatura de exposição na degradação do concreto em função da resistência à compressão e velocidade de propagação de onda ultrassônica

Euler Wagner Freitas Santos[a,b]
Débora de Almeida Nunes[a]
Carlos Otávio Damas Martins[a]
Michael Douglas Santos Monteiro[c]
Cochiran Pereira dos Santos[d]
Eliana Midori Sussuchi[c]
Sandro Griza[a]

[a]Universidade Federal de Sergipe – UFS, Programa de Pós-Graduação em Ciência e Engenharia de Materiais – P²CEM, São Cristóvão, SE, Brasil
[b]Instituto Federal de Sergipe – IFS, Coordenação de Engenharia Civil – COEC, Aracaju, SE, Brasil
[c]Universidade Federal de Sergipe – UFS, Programa de Pós-Graduação em Química – PPGQ, São Cristóvão, SE, Brasil
[d]Universidade Federal de Sergipe – UFS, Departamento de Física – DFI, São Cristóvão, SE, Brasil

Received 12 May 2022
Accepted 16 March 2023

Abstract: This study evaluated the influence of heating temperature variability on the degradation level of concrete by varying the exposure temperatures (200°C, 450°C, and 800°C) and concrete design strength (C25 and C40). The concretes were submitted to ultrasound tests (before and after heating) and then were ruptured by axial compression. After rupture, samples were taken from the fracture section of the specimens for microstructural analysis by scanning electron microscope (SEM), and molecular analysis by Raman spectroscopy. The results showed that the residual strength of the concrete can change significantly (values differing by more than 100%) with temperature variability in the oven. There were physicochemical changes in the concrete constituents. The variations in Raman spectra and morphological changes (SEM images) allowed to analyze the variation in the level of degradation of concrete after exposure to fire, at the same firing step, due to temperature variation in the ovens, being compatible with the results of compressive strength and ultrasonic wave propagation velocity (UPV). Thus, the study highlights the need for adequate mapping of the heat in the oven and monitoring of the temperature of specimens in studies of concrete at high temperatures.

Keywords: degradation, concrete, temperature variation, residual strength.

Resumo: Este estudo avaliou a influência da variabilidade da temperatura de aquecimento no nível de degradação de concretos, variando-se temperatura de exposição (200°C, 450°C e 800°C) e resistência de projeto do concreto (C25 e C40). Os concretos foram submetidos a ensaios de ultrassom (antes e depois do aquecimento), e, posteriormente, foram rompidos à compressão axial. Após a ruptura foram retiradas amostras da seção de fratura dos corpos de prova para análises microestruturais, por microscópio eletrônico de varredura (MEV), e análises moleculares, por espectroscopia Raman. Os resultados mostraram que a resistência residual dos concretos pode mudar de maneira significativa (valores divergindo em mais de 100%) com a variabilidade de temperatura no forno. Houve alterações físico-químicas dos constituintes do concreto. As variações nos espectros Raman e as alterações morfológicas (imagens em MEV) permitiram verificar a variação do nível de degradação do concreto após exposição ao fogo, em uma mesma etapa de queima, devido variação de temperatura nos fornos, sendo compatíveis com os resultados de resistência à compressão e

Corresponding author: Euler Wagner Freitas Santos. E-mail: euler.wagner@ifs.edu.br
Financial support: None.
Conflict of interest: Nothing to declare.
Data Availability: The data that support the findings of this study are available from the corresponding author [E.W.F Santos], upon reasonable request.

com os de ultrassom (velocidade do pulso ultrassônico). Dessa forma, o estudo evidencia a necessidade do mapeamento adequado do calor no forno e do monitoramento da temperatura dos corpos de prova, em estudos sobre concretos sob altas temperaturas.

Palavras-chave: degradação, concreto, variação de temperatura, resistência residual.

How to cite: E. W. F. Santos et al., "Influence of exposure temperature variability on concrete degradation as a function of compressive strength and ultrasonic wave propagation velocity," *Rev. IBRACON Estrut. Mater.*, vol. 17, no. 1, e17104, 2024, https://doi.org/10.1590/S1983-41952024000100004

1 INTRODUCTION

Concrete is recognized for its good performance at high temperatures [1]–[5], due to its incombustibility and low thermal conductivity [1]; in addition, the greater dimensional robustness of reinforced concrete structural elements makes them fire-resistant for a longer time compared to those made with other materials [1], [2]. Nevertheless, the constituents of concrete (cement paste and aggregates) decompose with heat, which not only influences the mechanical strength but also interferes with the modulus of elasticity and thermal properties of concrete [1], [2], [5]–[7].

Regarding the hydrated cement paste phase, the main solid products of cement hydration, which have a relevant influence on paste and concrete properties in fire, are calcium sulfoaluminates (ettringite: C-A-S-H); calcium silicate hydrate (C-S-H), the most important phase that defines the paste properties; and calcium hydroxide ($Ca(OH)_2$ - portlandite: CH) [1], [5], [6], [8]–[11]. In fire situations, their decomposition occurs at different temperatures and affects the integrity of reinforced concrete structures [1], [6], [8], [9], [12].

The temperature rise in fire situations generates temperature gradients, moisture variations, and crystalline transformations that induce structural and dimensional changes in the micro and macrostructure of concrete [7], [8]. Microstructural changes can be traced through characterization techniques such as the molecular analysis by Raman spectroscopy, used in this study to follow the different changes in the chemical compounds of concretes after exposure to high temperature [13]–[15], at the same firing step in the oven, especially of the CSH. Morphological studies of the microstructure of post-fire concrete by scanning electron microscopy (SEM), have also been efficiently used to analyze concrete degradation [6], [10]–[12].

This thermal gradient mentioned above causes these transformations in the material to vary according to the depth of the surface exposed to fire [1], [9], [10], as shown in the curves by Ongah et al. [16]. As concrete is not a good thermal conductor, the heat propagation process inside it is slow [1], [9], [10], [17], [18].

Studies involving concrete in fire situations are carried out considering external thermal actions with heat flow by convection or radiation from the hot gases of the burning environment [1], [3], [17], [18]. Fire curves are standardized for use in fire resistance studies with building materials and serve as a parameter in structural designs. The most widely adopted curve in Brazil for simulating concrete fire scenarios is ISO 834 [1], [3], [19]. For design purposes, it is common practice to admit that the temperature of the burning environment reaches its maximum value and that there is a uniform temperature distribution in the room [3], [17]. However, in a real fire, there is the variability of exposure to fire in structural elements [17], [20], [21], due to the greater or lesser amount of heat absorbed from fire or smoke [18], [20], [21], which results in the variation of degradation of the structures of concrete and structural elements [20], [21].

Similarly, large degradation differences may occur between concrete specimens under the same firing process due to temperature variability in the oven, although Akca and Özyurt [10] emphasize that, under the same heating scenario, the temperature gradient and the maximum temperature reached in concrete specimens are larger than in real structural elements.

Another factor to be highlighted is that many studies regarding fire simulation in concrete are carried out with young concrete, in which the moisture content is relatively high and the degree of hydration is reduced, which may be premature for fire simulation [1], [8], [22]. Britez [22] proposes that studies with concrete at high temperatures be carried out with at least one year of age of the material when it is expected that the concrete subjected to the heat of the fire is more compatible with the concrete of existing buildings and in full use.

In the evaluation of microstructural techniques used in the stages of inspection and recovery of post-fire reinforced concrete structures, Fernandes et al. [23] point to the lack of standardized procedures.

Some studies have shown the efficiency of ultrasound in evaluating post-fire concrete structures [24]–[26]. The analysis of the level of degradation of the concrete occurs by observing the reduction of the ultrasonic pulse velocity (UPV) after heating. In the study by Alcaino et al. [25], ultrasound proved to be a very effective tool in the inspection of post-fire reinforced concrete structures, allowing diagnoses that are not restricted to visual inspection.

Associating non-destructive field tests with microstructural analyses [11], [14], [24]–[26], reliable results can be obtained to identify both the level of damage to structural elements and the level of concrete degradation.

Given the above, in order to contribute to the analysis of damage caused by exposure of concrete to high temperatures [1], [3], [26], this study investigates the variation of degradation of concrete specimens due the variation of temperature at specimens, in the same burning process. This can lead to quite different information from that obtained when only considering the analysis of mean values of post-fire tests on concrete samples. The concrete specimens were heated at an age of 720 days.

In order to do so, the results of ultrasonic tests will be compared with the results of mechanical tests of axial compressive strength, correlating them with the results of molecular analysis by Raman spectroscopy [13]–[15] and also with those of microstructural morphological studies by scanning electron microscope (SEM) [6], [11], [12]. All involving concretes of two strength classes (variation of the water/cement ratio) submitted to three testing temperatures.

2 MATERIALS AND EXPERIMENTAL PROGRAM

2.1 Materials

The inputs used in the production of concrete were subjected to the characterization tests shown in Table 1. The definition of these properties is relevant for both the understanding of the thermal behavior of aggregates [1], [5], [9], [12], [27]–[29] and for the concrete mix design procedures [4], [5]. The polyfunctional additive (Muraplast FK 320) and the hydration stabilizer additive (Hydrakem Novakem) were also used in the mixture of the two types of concrete used in this study. The water used in the mixture was from the local water distribution network.

Table 1. Results of the physical characterization.

Inputs	Characterization test		
	Fineness (ABNT NBR 11579:2012)	**Hot expandability (ABNT NBR 11582:2018)**	**Initial setting time (ABNT NBR 16607:2018)**
Portland Cement CP II F 40	Fineness index= 6.3%	0.3 mm	75 minutes
	Real specific mass (ABNT NBR 16917:2021)	**Unit mass (ABNT NBR 16972:2021)**	**Granulometry (ABNT NBR NM 248:2003)**
Fine-grain natural fine-sand aggregate	2.605 g/cm^3	1.930 g/cm^3	Dmax = 2.4mm
Artificial gneiss fine-sand aggregate	2.667 g/cm^3	1.300 g/cm^3	Dmax = 2.4mm
Coarse aggregate (gnaisse)	2.643 g/cm^3	1.400 g/cm^3	Dmax = 12.5mm

2.2 Production of specimens

The two classes of concrete strength used in this study, Class C25 and C40 (NBR 8953 [30]), were adopted because they are common in reinforced concrete structures. In the concrete mixture, the proportionality between the constituents (mix design) followed the official document provided by the concrete company, including the water/cement ratio, which was 0.65 and 0.53 for the concretes of classes C25 and C40, respectively.

After mixing, the concrete cylindrical specimens (100 mm x 200 mm) were molded following the procedures of NBR 5738 [31]. After 24 hours, they were removed from the molds and taken to moist curing by immersion for 30 days [32]–[34], from where they were left for air drying until the age of fire exposure. Twenty specimens were molded for each of the strength classes addressed in this study (five not exposed to fire and fifteen exposed to temperatures of 200 ºC, 450 ºC, and 800 ºC).

In order to verify the physical-chemical transformations that occur in the material [6], [9], [10], and therefore, the effects on the mechanical properties of concrete, especially compressive strength, the specimens were subjected to exposure to fire at an age of 720 days. Which is in accordance with Britez and Costa [1] and predicted in RILEM [32], [33], regarding the need for studies on concrete against fire to meet the minimum requirements of maturity, moisture, and hydration degree. For each of the strength classes, the fifteen heated specimens formed three control groups, each group containing five specimens that were exposed to each temperature level previously mentioned. Another control group was formed by the five specimens that served as reference, for each strength class, so they were not heated and were used to verify the axial compressive strength of concrete at room temperature and at the heating age. The control groups were defined as follows: groups 25REF, 25200, 25450, and 25800, which are concretes of strength class C25, reference specimens and at temperatures of 200 °C, 450 °C, and 800 °C, respectively; groups 40REF, 40200, 40450, 40800, which are concrete of strength class C40, reference specimens and at temperatures of 200 °C, 450 °C, and 800 °C, respectively.

2.3 Heating and cooling of specimens

The specimens were heated in a ceramic block firing oven (Figure 1) from a ceramic products industry. The monitoring of the temperature on the surface of the samples was done using pyrometers (model MT 395 A -MINIPA) and infrared camera (FLIR- series T- model T-640)-Figure 1c. In the oven, the concretes were exposed to fire until reaching the target temperatures of 200 °C, 450 °C, and 800 °C.

Due to the thermal treatment time adopted, during each firing stage it was possible to observe temperature variability inside the oven, and, consequently, in the concrete specimens, as occurs with the structural elements of buildings in fire situations, where, due to greater exposure to heat, some elements, or part of them, are more degraded [16], [17], [19], [20]. At each stage of exposure to fire, temperature readings were taken in at least six specimens, resulting in the mean temperatures and standard deviations shown as follows: for the target temperature of 200 °C the average temperature was 188 °C and the standard deviation was 58 °C; for the target temperature of 450 °C they were 401 °C and 52 °C, respectively; for the target temperature of 800 °C they were 778 °C and 156°C, respectively. Confirming that there was this temperature variability between the specimens, and, therefore, variation of degradation, even with the procedures described above.

After 100 minutes of the specimens reached the target temperature predicted in each firing step, all specimens were removed from the oven and cooled in the air until they reached room temperature, as shown in Figure 1d.

In the present study it was decided to limit the exposure time, which leads to temperature gradients along the section of the specimens. This was done so as not to expose the surfaces to too much heating time, thus allowing both the curves performed by Ongah et al. [16] to be met, and the tests and analyses proposed in this study to be performed, based on the size of the standardized specimens used. Furthermore, even if a longer exposure time was used, it was expected that there would be a degradation gradient of the specimens, due to the temperature difference between the core region and its surface.

The reference specimens, at the heating age of the other specimens, had their moisture content determined by the conventional weighing procedure, obtaining their weight before and after being placed in the oven where they remained for 24 hours at a temperature of 100 ºC. The average moisture obtained was 2.12% for class C25 concrete and 2.48% for class C40.

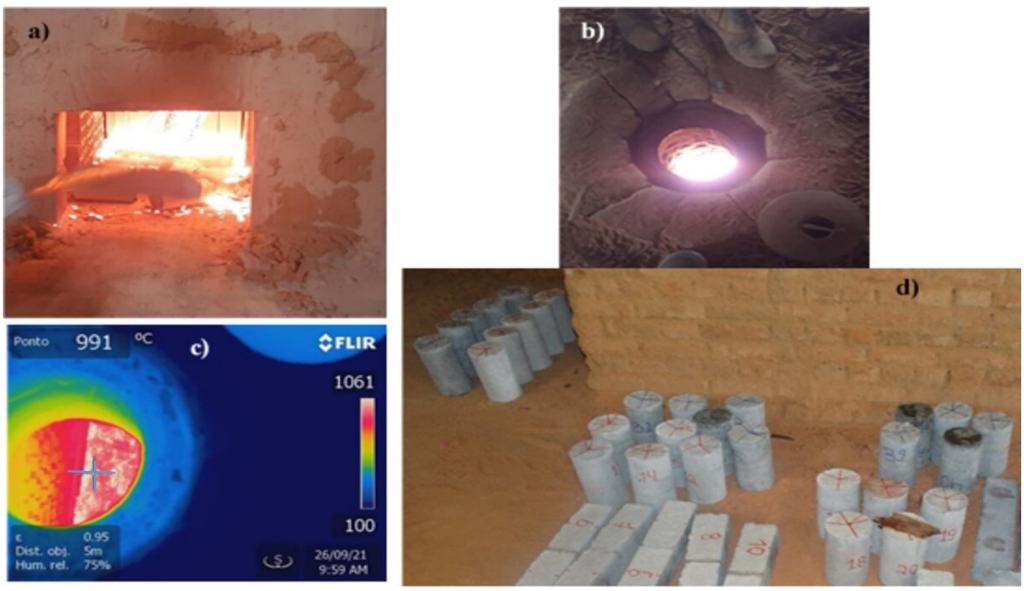

Figure 1. Ceramic industry oven used to heat the specimens: a) access window in the oven door; b) upper opening of the oven; c) thermal image of concrete specimens in the oven; d) specimens cooling after leaving the oven.

2.4 Axial compression test

All concrete specimens were subjected to the axial compressive strength test (Figure 2), as defined by NBR 5739 [34]. These tests occurred in the mechanical testing machine MUE-100 (load capacity of 100 tf). Of the forty specimens tested, thirty were ruptured after being heated in the oven, and ten were reference specimens. The rupture of these specimens made it possible to verify the variation of the residual strength of the concrete, after the same firing step, due to the non-uniformity of heat in the oven. This can also be confirmed by the variation of ultrasound signals, by the results of Raman spectroscopy, and by the microstructure images present in the samples analyzed by SEM.

Figure 2. Specimen during compression rupture test.

2.5 Ultrasound tests

The concrete specimens were subjected to direct measurements of the ultrasonic pulse velocity (UPV) with PUNDITLAB ultrasound, 54 kHz transducer, before and after being heated in the oven (Figure 3). In these procedures, the recommendations of RILEM [35] were followed. These measurements allowed to evaluate the variation of UPV, in post-heating, between specimens of the same control group, and therefore, submitted to the same firing step in the oven. In addition, they allowed to correlate the variation of these velocities with the variation of the results of destructive tests of mechanical compression, in concrete from the same control group.

Figure 3. Specimens during measurement of ultrasonic pulse velocity.

2.6 Analysis of the microstructural morphology of concrete after exposure to fire

Samples were collected from the fracture surface of specimens submitted to the same firing process (same control group) for evaluation by scanning electron microscope (SEM -JCM-5700 CARRY SCOPE), after drying in the oven for 24 hours (at 100 °C) and gold plating. These analyses allowed visualizing different morphological changes in the microstructure of the concrete specimens belonging to the same control group, as a function of the variability of the oven temperature, which incurs in the variation of degradation of concrete subjected to the same firing process.

Scanning the sample using SEM makes it possible to identify the presence or absence of the characteristic microstructures of the main cement hydration products [5], [12], [36], the state of deterioration of aggregates [11] and, thus, better estimate the level of severity of the fire on the concrete [11], [12], [23]. The samples were taken from the fracture surface from points located up to 2 cm from the edges, in order to ensure that the concrete reached the target temperature, according to Ongah et al. [16].

2.7 Verification of chemical compounds in concrete

Raman spectroscopy was used on samples obtained from the fracture surfaces of specimens exposed to fire in the same firing - at least three concrete samples from each control group were used. This characterization technique contributes to the identification of cement hydration products and aggregate phase changes making it possible to estimate the temperature reached by the concrete [11], [13]–[15], [36]–[42]. The same methodology was used for choosing samples for analysis by Raman spectroscopy and SEM. However, in the Raman spectroscopy technique, data were collected from at least three points in each sample, in order to minimize the effects of eventual sample inhomogeneity, and then averaged to create a Raman profile for all the concrete samples.

The Raman spectra of the samples were obtained with the Dispersive Raman Spectroscopic Senterra, Bruker Optik GmbH. The analyses were performed on two solid powder samples, which were deposited on glass slides, and extracted from the fracture surface of concrete specimens after the axial compression failure test. The scans were performed using an iodine laser with a wavelength of 785 nm, in the region from 100 to 1600 cm^{-1}.

In the present study, Raman spectroscopy has contributed to identifying the differences in the degradation of concrete specimens submitted to the same heating step, through the temperature variability in the oven. Confirming what was observed in the micrographs, the Raman spectra obtained showed a variation in the chemical compounds present in samples extracted from concretes belonging to the same control group, i.e., which were submitted to the same firing instant.

3 RESULTS AND DISCUSSIONS

3.1 Ultrasonic pulse velocity variation (UPV)

The results of the ultrasonic pulse velocities (UPV) shown in Table 2 correspond to those measured before and after exposure of the concrete specimens to fire, for both the concretes of class C25 strength and for those of class C40.

As shown in Table 2, for both strength classes, there was a reduction in the average UPV with increasing temperature, as predicted in the literature [24]–[26]. This can also be observed from the average velocities of specimens before and after exposure to fire, as shown in Table 2. The comparison of UPV averages is shown in Table 3. By applying the statistical treatment of Student's t-test, with 95% confidence, there was significant variation (t>critical and P factor <0.05) of UPV for specimens heated up to the three temperature ranges treated in this study, except in class C25 for the temperature of 450°C. Which may result from the greater dispersion of the values in relation to the average velocities at this temperature.

Table 2. Results of ultrasonic wave velocity in C25 e C40 concrete, in m/s.

Strength Class	Before heating (V_0)			After heating (V_0)		
	C25200*	C25450*	C25800*	C25200	C25450	C25800
C25	4516.65	4346.75	4654.00	4190.18	3284.56	3541.42
	4493.09	4597.26	4476.35	4159.18	4041.21	1953.56
	4540.84	4593.85	4593.54	4240.10	3295.78	1940.23
	4627.03	3509.03	4522.85	4255.60	3983.39	357.48
	4555.10	4573.39	4648.11	4079.65	2221.12	744.09
Average	**4546.54**	**4324.06**	**4578.97**	**4184.94**	**3365.21**	**1707.36**
Coefficient of variation (%)	**1.12**	**10.81**	**1.70**	**1.68**	**21.83**	**73.09**
C40	5017.37	4986.36	5075.65	4680.35	2710.05	3812.55
	4884.98	4905.13	4923.12	4442.55	3954.55	1952.32
	4865.76	4934.59	4910.09	4452.79	2439.39	2204.38
	4891.80	4973.03	5024.50	4505.80	4653.38	3672.11
	4924.67	4935.21	4960.63	4547.66	4193.90	235.63
Average	**4916.91**	**4946.86**	**4978.80**	**4525.83**	**3590.26**	**2375.40**
Coefficient of variation (%)	**1.22**	**0.66**	**1.41**	**2.13**	**26.88**	**61.49**

*Readings of the specimens before heating.

Table 3. Statistical indicator for test t of student-comparative UPV before and after heating.

Strength class	Comparative *	Factor t	P-value	tcritical
C25	V_0 200: Vθ 200	11.81	29.46E-5	2.78
	V_0 450 - Vϴ 450	2.07	0.10700	2.78
	V_0 800 - Vϴ 800	5.24	6.34E-4	2.78
C40	V_0 200 - Vϴ 200	22.10	2.48E-5	2.78
	V_0 450 - Vϴ 450	3.13	0.03500	2.78
	V_0 800 - Vϴ 800	4.11	0.01470	2.78

*See the corresponding values in Table 2.

KVθ is defined as the coefficient of reduction of the concrete UPV velocity according to the increase of the exposure temperature, obtained according to Equation 1.

$$KV\theta = V/V_0 \quad (1)$$

Where V_0 = average ultrasonic pulse velocity of the specimens before heating to the target temperature θ (m/s); V= ultrasonic pulse velocity of each specimen heated at the temperature θ (m/s).

The KVθ values in Table 4, for each temperature in question, were obtained by averaging the values of this coefficient for each specimen. The coefficients of variation of these coefficients, corresponding to each control group, are also described in this table.

Table 4. Velocity reduction factor (KVθ) for classes C25 e C40.

Strength class	C25			C40		
Control group	C25200	C25450	C25800	C40200	C40450	C40800
KVθ	0.92	0.78	0.37	0.92	0.73	0.48
Coefficient of variation (%)	1.63	21.90	72.97	2.07	27.40	60.42

Aiming to evaluate the behavior of the reduction of KVθ values with the exposure temperature, the statistical treatment of Anova - double factor with repetition was used, considering a 95% confidence level. The F-value and the significance probability (P-value), presented in Table 5, indicate that the variation of the KVθ coefficient with the increase of the temperature is significant, however, the same does not occur by changing the strength class of the concrete (in the line "sample", F<Fcritical and P-value>0.05). The reduction of the velocity is independent of the strength classes studied. To determine which averages of these coefficients are statistically different, with a confidence level of 95%, the Tukey test was performed, as shown in Table 6.

Table 5. Statistical indicators for ANOVA-double factor with repetition for the velocity reduction factor (KVθ).

Source of variation	SQ	DF	MQ	F	P-value	F critical
Sample	0.002231	1	0.002231	0.059	0.811	4.260
Columns	1.269401	2	0.634701	16.71	2.84E-05	3.403
Interactions	0.031819	2	0.015909	0.419	0.663	3.403
Within	0.911597	24	0.037983			
Total	2.215048	29				

SQ=Sum of squares (total); DF=degree of freedom (total); MQ= Mean Square (Variance)

The pairs analyzed in Table 6 indicate that the difference between the means of KVθ at temperatures of 200 °C and 800 °C is greater than the minimum significant difference (MSD) for both concretes under study. Between temperatures of 450 °C and 800 °C, this difference occurs only in class C25. For both strength classes, the reductions of UPV at temperatures of 200 °C and 450 °C are equal.

Table 6. Comparison between the UPV averages (Tukey's test) with respective minimum significant differences (MSD) for each pair.

Class of concrete	Comparative *	MSD	Difference between averages	Conclusion
C25	C25200 - C25450	0.308	0.142	equals
	C25200 - C25800	0.308	0.548	different
	C25450 - C25800	0.308	0.405	different
C40	C40200 – C40450	0.308	0.195	equals
	C40200 – C40800	0.308	0.443	different
	C40450 – C40800	0.308	0.249	equals

*See the corresponding values in Table 4.

Table 2 shows that there is a higher coefficient of variation between UPV values in the control groups for the temperature levels of 450 ºC, and 800 °C for both strength classes. This also confirms the greater influence of the variability of the oven temperatures on the degradation levels of the concretes at these exposure temperature levels.

In order to evaluate the variation of concrete degradation at temperatures of 450 ºC and 800 °C, observing the influence of non-uniformity of heat in the oven, the parameter KVθ1 was defined as the velocity reduction coefficient obtained from the specimen with the lowest UPV value in post-heating, according to Equation 2.

$$KV\theta 1 = V_1/V_0 \quad (2)$$

Where V_0= average velocity of the specimens before heating to θ (m/s); V_1= the minimum velocity of the specimen heated to θ (m/s).

Table 7 shows the KVθ1 values for the temperature levels under study, considering the strength classes C25 and C40. In both classes there are lower values of residual velocities at temperatures of 450 °C and 800 °C, compared to what was observed at these temperature levels in Table 4, indicating that there may be sudden variation in the degradation of concrete specimens due to the higher or lower exposure to heat in the same firing. In addition, it is noted that the non-uniformity of temperature in the oven, at the highest heating levels (450 °C and 800 °C), caused a greater variation in concrete degradation.

Table 7. KVθ1 coefficients for classes C25 e C40.

Class		**C25**			**C40**	
Group	C25200	C25450	C25800	C40200	C40450	C40800
KVθ1	0.92	0.51	0.08	0.92	0.49	0.05

3.2 Compression strength of concrete

Table 8 shows the values of compressive strength of concrete specimens, both reference specimens (not exposed to fire) and those submitted to heating at the three exposure temperatures considered. There was a decrease in the average strength value with increasing temperature, in accordance with the literature [3], [9], [25].

Table 8. Compressive strength results for C25 and C40, in MPa.

Control group	**Compressive strength – Rθ**						
			C25			**Average**	**Coefficient of variation (%)**
C25REF	34.15	24.67	35.25	28.14	33.74	31.19	14.65
C25200	25.69	33.88	33.85	35.55	25.03	30.80	16.30
C25450	14.87	25.76	26.34	31.26	23.44	24.33	24.70
C25800	24.57	14.55	18.99	17.33	18.70	18.83	19.44
Control group			**C40**			**Average**	**Coefficient of variation (%)**
C40REF	45.67	52.44	50.00	54.01	52.66	50.96	6.46
C40200	53.91	46.82	50.35	49.26	52.60	50.59	5.51
C40450	37.25	41.20	32.26	51.10	50.88	42.54	19.61
C40800	48.78	21.58	29.46	34.71	10.87	29.08	48.87

KCθ is defined as the coefficient of reduction of the axial compressive strength of concrete by increasing the exposure temperature (Equation 3).

$$KC\theta = R/R_0 \quad (3)$$

Where R_0= Average strength of the reference specimens (MPa); R= strength of each specimen heated to θ (MPa).

The KCθ values shown for each temperature level in Table 9 were obtained by averaging the values of this coefficient for each specimen. The coefficients of variation of these coefficients, corresponding to each control group, are also described in this table.

Table 9. Axial compression strength reduction factor (KCθ) for classes C25 e C40.

Class		**C25**				**C40**		
Group	C25REF	C25200	C25450	C25800	C40REF	C40200	C40450	C40800
KCθ	1	0.99	0.78	0.60	1	0.99	0.83	0.57
CV* (%)	-	16.16	24.36	20.00	-	5.05	19.28	49.12

*CV= Coefficient of variation

In order to evaluate the behavior of the reduction of KCθ values with the exposure temperature, it was used the statistical treatment of Anova - double factor with repetition, considering a 95% confidence level. The F-Values and the significance probability (P-value), presented in Table 10 indicate that the variation of the mean of the KCθ coefficients with the increase of the temperature is significant, but the reduction of strength is independent of the classes of concrete strength (in the line "sample", F<Fcritical and P-value>0,05). Which is analogous to what occurred with the reductions of UPV.

To determine which means of these coefficients are statistically different, with a confidence level of 95%, Tukey's test was performed (Table 11).

Table 10. Statistical indicators for ANOVA-double factor with repetition for axial compression strength factor (KCθ).

Source of variation	SQ	DF	MQ	F	P-value	Fcritical
Sample	0.000423	1	0.000423	0.018	0.893	4.14910
Columns	1.131994	3	0.377331	16.330	1.30E-06	2.90112
Interactions	0.009970	3	0.003323	0.144	0.933	2.90112
Within	0.739437	32	0.023107			
Total	1.881800	39				

SQ=Sum of squares (total); DF=degree of freedom (total); MQ=Mean Square(variance).

The pairs analyzed in Table 11 show that the difference between the averages of KCθ at temperatures of 200 °C and 800 °C is greater than the minimum significant difference (MSD), for both concretes under study, there is, therefore, reduction of resistance with heating at this temperature level. The same occurs in the comparative KCθ between the temperatures of 800 °C and room temperature. There was no significant reduction in concrete strength for heating up to temperatures of 200 °C and 450 °C for both strength classes. The strength reduction coefficients at these two temperatures are, according to the statistical treatment adopted, equal to those at room temperature (groups C25REF and C40REF).

Table 11. Comparison between the average values of KCθ (Tukey's test) and the minimum significant difference (MSD) for each pair.

Strength Class	Comparative *	MSD	Difference between averages	Conclusion
C25	C25REF - C25200	0.261	0.012504	equals
	C25REF - C25450	0.261	0.219814	equals
	C25REF - C25800	0.261	0.396345	different
	C25200 - C25450	0.261	0.20731	equals
	C25200 - C25800	0.261	0.383841	different
	C25450 - C25800	0.261	0.176531	equals
C40	C40REF – C40200	0.261	0.007222	equals
	C40REF – C40450	0.261	0.165201	equals
	C40REF – C40800	0.261	0.430211	different
	C40200 – C40450	0.261	0.157980	equals
	C40200 – C40800	0.261	0.430211	different
	C40450 – C40800	0.261	0.265010	different

*See the corresponding values in Table 9.

The results obtained for the temperature of 450ºC are diverging from the technical literature [5], [6], [9], [11]–[13], [43] that reports a reduction in strength at this level of concrete heating due to the partial decomposition of CSH and portlandite. Tables 8 and 9 show a higher coefficient of variation for compressive strength and KCθ values, respectively, in the two control groups corresponding to this temperature level (C25450 and C40450). This fact should indicate a greater influence of temperature variability in the oven in this firing, and, consequently, variation in the degradation of the concretes, even if the deviation observed in the oven at this temperature (450 °C) was lower than at the temperature of 200 °C (item 2.3). This is due to the little decomposition of the constituents responsible for the strength of the concrete at this lower temperature level (200°C).

In line with what was discussed in the UPV reduction analysis (item 3.1), also at the temperature of 800 °C, there is a greater coefficient of variation between the values of compressive strength for both strength classes, indicating a greater influence of the non-uniformity of temperature in the oven in the degradation of the specimens during heating at this temperature level.

The parameter KCθ1, defined as the strength reduction coefficient for the specimen with the lowest value of compressive strength after heating (Equation 4), was used to contribute to the evaluation of the influence of temperature variability in the oven on the variation of concrete degradation, especially at temperatures of 450 °C and 800 °C.

$$KC\theta 1 = R_1/R_0 \quad (4)$$

Where R_0= Average axial compression strength for the reference specimens (MPa); R_1= Minimum axial compression strength for specimens heated to θ (MPa).

The values of KCθ1 for the temperatures under study, in classes C25 and C40, are presented in Table 12. Especially at temperatures of 450 °C and 800 °C, the values of residual strength observed point to a large variation in the degradation of concrete specimens due to the higher or lower exposure to heat in the same firing, as also seen from the variation of the residual velocity. This also confirms the previous statement about at higher temperatures - 450°C and 800°C (item 2.3), there is a greater influence of the temperature variation in the oven, on the levels of degradation of the specimens.

Table 12. KCθ1 coefficients for classes C25 e C40.

Class		**C25**			**C40**	
Group	C25200	C25450	C25800	C40200	C40450	C40800
KCθ1	0.80	0.48	0.47	0.92	0.63	0.21

3.3 Residual strength *versus* residual velocity

3.3.1 Average residual compressive strength (KCθ) *versus* average residual velocity (KVθ)

Table 13 presents, for the two strength classes under study, both the average values of the velocity reduction coefficients (KVθ) and compressive strength (KCθ), as well as the values of these coefficients for the specimens with lower velocity and strength, KVθ1 and KCθ1, respectively.

Table 13. KVθ, KVθ1, KCθ e KCθ1 coefficients for classes C25 e C40.

Class		**C25**			**C40**	
Group	C25200	C25450	C25800	C40200	C40450	C40800
KCθ	0.99	0.78	0.60	0.99	0.83	0.57
KCθ1	0.80	0.48	0.47	0.92	0.63	0.21
KVθ	0.92	0.78	0.37	0.92	0.73	0.48
KVθ1	0.92	0.51	0.08	0.92	0.49	0.05

Figure 4 shows the graph with the average reduction coefficients (KVθ and KCθ), for classes C25 and C40, as well as the correlation curve of residual strength *versus* residual velocity. By the trend line that it is possible to state that there is a linear relationship between resistances and residual velocities, once the determination coefficient in the linear regression (R^2) is higher than 0.94, indicating that the adopted model is well-adjusted to the data. It is observed that the average residual strengths and velocities tend to decrease with the increase of temperature, with the same behavior for the two concretes under study, although until the temperature of 450 °C the values of residual strengths are statistically equal, as discussed in item 3.2. This behavior is identical to the residual velocities, as discussed in item 3.1.

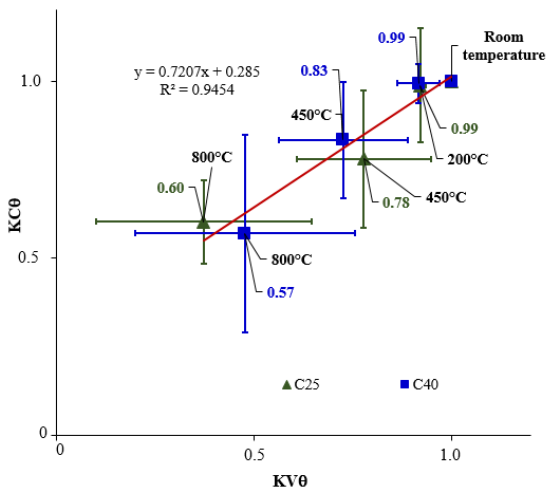

Figure 4. Correlation curves of KCθ *versus* KVθ for C25 e C40.

3.3.2 Minimum residual strength (KCθ1) *versus* minimal residual velocity (KVθ1)

The graph with the reduction coefficients referring to the specimens with lower velocities and residual strengths (KVθ1 and KCθ1), for classes C25 and C40, is presented in Figure 5. It also shows the correlation curve of the lowest residual strength versus lowest residual velocity, through which it is also possible to observe that there is a linear relationship between KVθ1 and KCθ1, with a linear regression coefficient of determination (R^2) of 0.89, indicating that the adopted model is also well fitted to the data. Similar behavior to that observed in the curve of Figure 4 is observed, with strengths and residual velocities reducing with increasing temperature, with both concretes presenting the same behavior. However, comparing the data from Figures 4 and 5, and those from Table 13, it can be seen that at 450 °C and 800 °C, the observed values for strengths and residual velocities indicate a greater variation in the degradation of the concrete specimens due to the variability of exposure to fire (item 2.3) during the same round of heating in the oven. There was a reduction in the residual strength, from KCθ=0.57 to KCθ1=0.21, and in the residual velocity, from KVθ=0.48 to KVθ1=0.05, at a temperature of 800 °C.

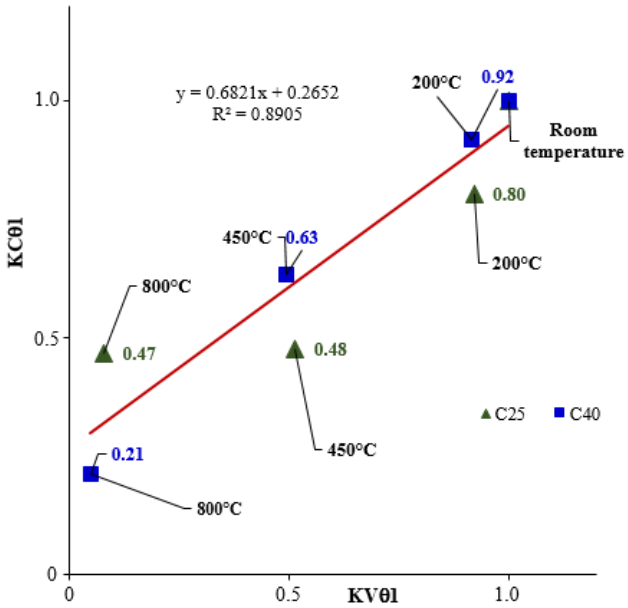

Figure 5. Correlation curve of KCθ1 *versus* KVθ1 for C25 and C40.

3.4 Material characterization

3.4.1 Scanning electron microscopy (SEM)

In the photographs obtained by scanning electron microscope (SEM), presented in Figure 6, it is possible to identify the difference between the morphology of compounds found in concretes that were submitted to the same firing step in the oven, with a target temperature of 450 °C. As expected in the technical literature [6], [9], [13], the micrograph of Figure 6a shows a lower prevalence of ettringite and monosulphates, as well as the presence of pores, CSH structures, and portlandite (CH), which is in line with what has been described in the literature [1], [6], [12], [13], [43], regarding the decomposition temperature range of portlandite (approximately 400 °C to 600 °C). In Figure 6b, the presence of ettringite needles and monosulphates is also observed, even though it was obtained from a concrete sample that was also submitted to the same heating moment corresponding to the target temperature of 450 °C.

The images shown in Figure 7 were obtained from concretes heated up to the target temperature of 800 °C, in the same firing step in the oven. In Figure 7a it is observed that the morphology of the compounds still characterizes the presence of portlandite (CH), but with the CSH quite decomposed in relation to what is observed in Figure 6a, although at this temperature level, the complete decomposition of portlandite was expected [7], [9], [11]–[13], [43]. In Figure 7b it is noted the highest degree of degradation of the sample analyzed since the greatest presence of voids is observed, with CSH structures in decomposition and greater difficulty to evidence the presence of portlandite (CH), justifying the greater loss of strength and UPV, observed in Figure 5, in the specimen corresponding to this concrete sample.

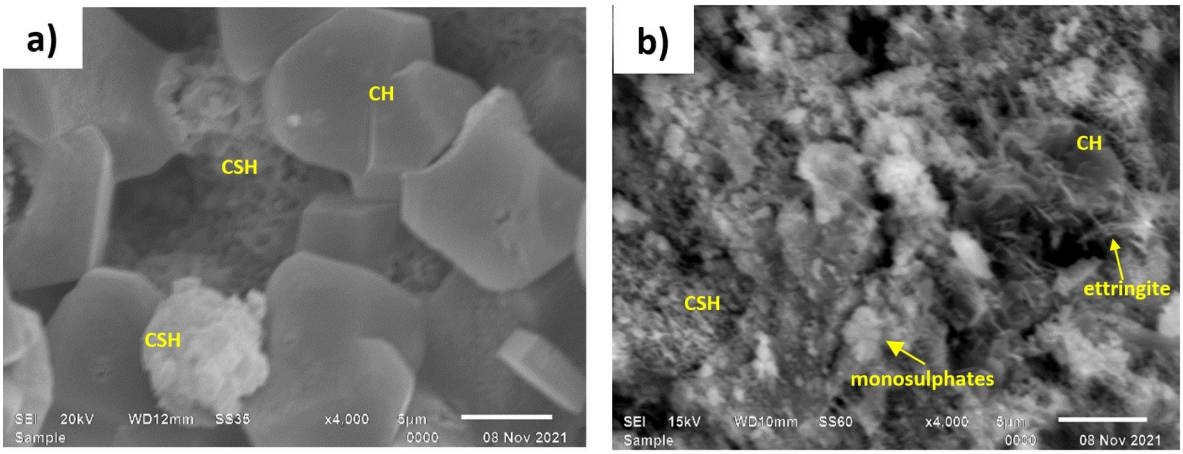

Figure 6. SEM micrographs of a concrete sample heated to 450°C: a) most degraded sample; b) less degraded sample.

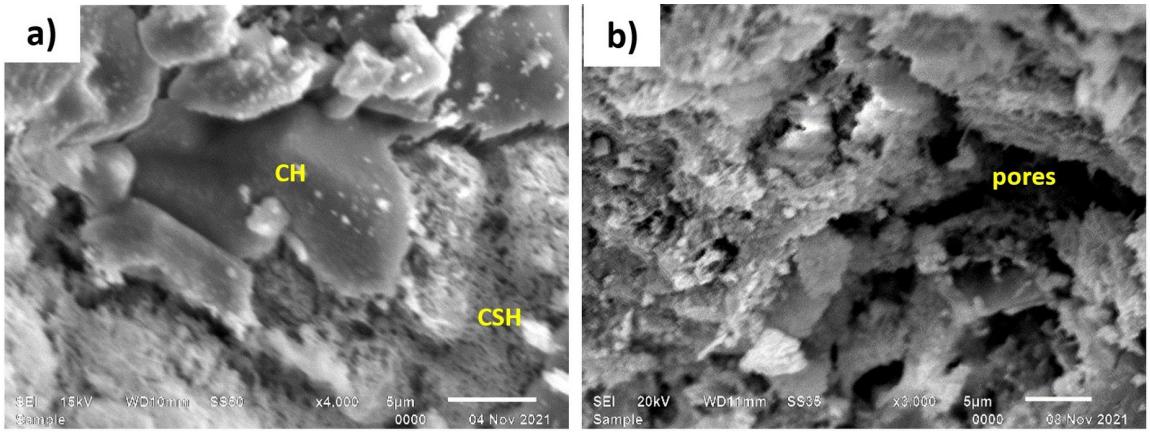

Figure 7. SEM micrograph of a concrete sample heated to a temperature of 800°C: a) less degraded sample; b) most degraded sample.

3.4.2 Raman spectroscopy

In the literature, some works emphasize the understanding of the structure of CSH, and its corresponding Raman shifts [13], [15], [38]–[41], from the relationship with the structure of tobermorite and jenite [13], [39], [41]. In it, the bands observed in the 800 to 1080 cm^{-1} are attributed to symmetric elongations of the Si-O tetrahedron. The band from 600 to 700 cm^{-1} corresponds to the symmetric bending of Si-O-Si. The spectral shift bands from 430 to 540 cm^{-1}, on the other hand, are associated with internal deformations of the Si-O tetrahedra in the O-Si-O bond. Finally, the bands in the range of 100 to 250 cm^{-1} are attributed to vibrations of Ca-O polyhedra [13], [39], [41].

Figure 8 shows the average Raman spectra of concrete subjected to the same firing process, heated at 450 °C and 800 °C. These spectra indicate the variation in the degradation of the concrete even though they were exposed to firing in the oven at the same time.

At 450°C, observing the three spectra of Figure 8a, besides the bands 3 of CSH [37]–[41], the band of portlandite (CH), at 365 cm^{-1} [13], [37]–[41], has less intensity in the blue curve in relation to the other two. There is a variation regarding the intensities of bands related to the decomposition products of CSH [6], [12], [13], [39], as can be observed by the formation of C_2S, at 533 and 614 cm^{-1}, of C_3S at 794 cm^{-1}, and of C_3A, at 753 cm^{-1} [13], [38], [40], [41]. There is also the most intense silica band at 465 cm^{-1} and the gehlenite band appears at 625 cm^{-1} [13], [38], only in the blue curve. Moreover, the absence of the band at 998 cm^{-1} [13], [38], [41], [42] indicates the decomposition of ettringite [1], [6], [9], [11]–[13], [43] in all samples. At this temperature, there were small shifts of the CSH bands among the three spectra, which, as predicted in the literature [13], [15], also suggests variation in CSH decomposition.

The analysis of these spectra confirms what was observed in the SEM images and in the residual strength and velocity curves since the sample corresponding to this blue curve is the concrete that presented the lowest KCθ and lowest KVθ.

Analyzing Figure 8b, temperature of 800 ºC, the appearance of a band in 465 cm^{-1} is observed in the red curve [12], [15], [38], [41], referring to the change of alpha quartz to beta quartz phase [1], [6], [9], [11], [13], [15], [42]. In it the bands related to CSH and portlandite [13], [3]–[41], are no longer present, indicating their decomposition, according to the literature [6], [9], [11]–[13], [15], [42]. This can also be proved by the existence of the gehlenite bands (at 614 and 908 cm^{-1} [38]) and the bands corresponding to the alite (C_3S) and belite (C_2S) phases [13], [38]–[41]. A slight shift and broadening of the base of the $CaCO_3$ band are observed, near 1080 cm^{-1}, which suggests an amorphous phase of this compound [13], [38], [40], [41].

In relation to the other spectra, the absence of portlandite-related bands is observed in all of them, but CSH and decomposition product bands are still present [13], [37]–[41], which indicates variation in the degradation of the concretes of these samples.

Thus, it is noted that the Raman spectrum of the sample corresponding to the red curve confirms what was observed through SEM images (Figure 7) and ultrasound results because this sample was extracted from the specimen with lower residual strength and velocity.

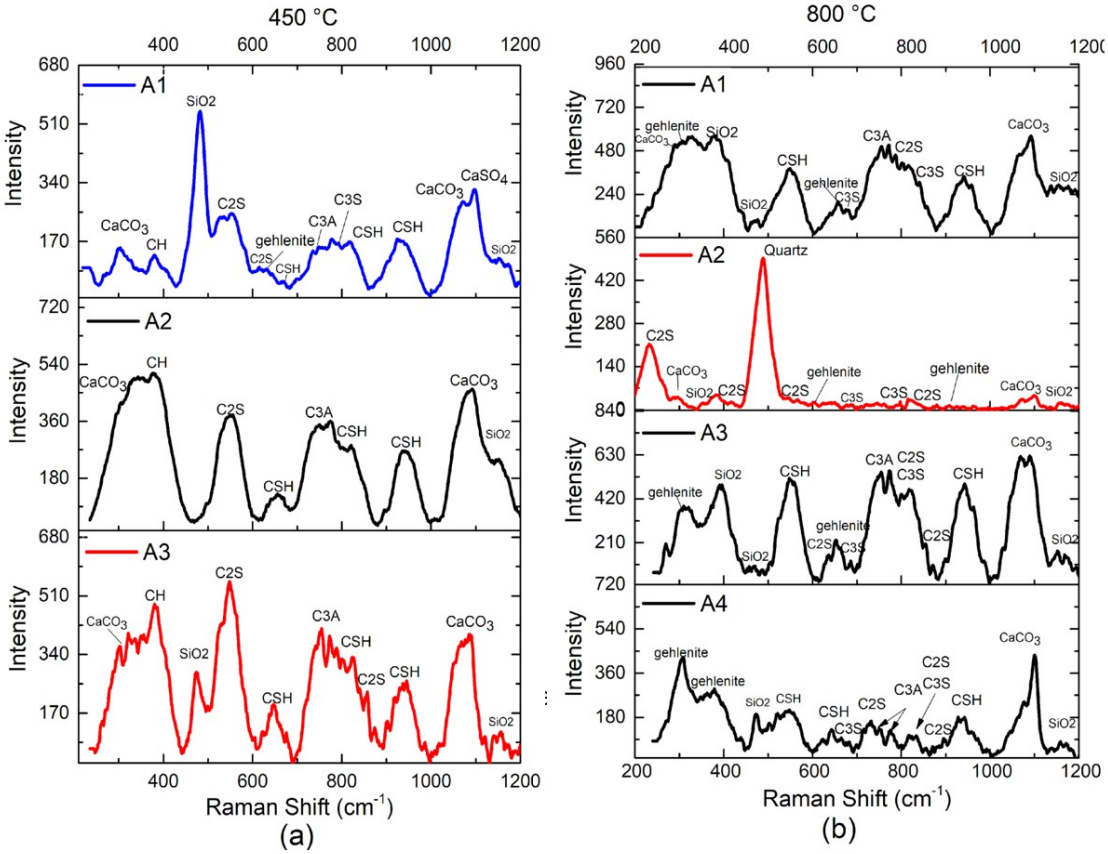

Figure 8. Raman spectra of concrete heated samples at 450°C (a) e 800°C (b).

4 CONCLUSIONS

The aim of this study was to evaluate the effectiveness of analyzing the level of degradation of concrete after exposure to fire by compressive strength and ultrasound results, by SEM analysis, and by Raman spectroscopy. The following conclusions can be drawn based on the results:

- Exposure to high temperatures causes physical-chemical changes in the concrete constituents, causing, therefore, a reduction in its compressive strength and ultrasonic pulse velocity (UPV), and this reduction is independent of the concrete strength class.

- The microscopic images showed different changes in the microstructure of the post-fired cement paste, depending on the higher or lower exposure to heat in the oven. The morphological changes were compatible with the results of compressive strength and UPV, contributing to the identification of the variation of concrete degradation by temperature variation in the oven.
- Raman spectroscopy allowed to verify the variation of the degradation level of concrete after exposure to fire, from the differences between the spectra obtained from concrete subjected to the same heating process. At 450°C, a variation in the intensity of the portlandite band was identified among the spectra, in addition to variations related to the intensity of the CSH decomposition products and displacements of its bands. At 800°C the degradation variation can be noted by the evidence of CSH bands in some spectra and the non-appearance of bands related to decomposition products, such as quartz.
- The temperature variability in the heating process caused differences greater than 100% between the average residual resistance (KCθ) and the one corresponding to the most degraded specimen (KCθ1), at the temperature of 800 °C. At this same temperature, the residual velocity of this most degraded specimen (KVθ1) was close to zero, while the average value (KVθ) was 48%.
- The temperature variability in the oven caused greater variation in degradation for the concretes heated up to the reference temperatures of 450 °C and 800 °C, which did not occur for the concretes exposed to heat at the target temperature of 200 °C.

ACKNOWLEDGEMENTS

The authors wish to thank the ceramics manufacturers Bom Bloco, Beton Engenharia Ltda and SENAI-SE, and the mixing plant Supermix. The authors are grateful to Brazilian development agencies Conselho Nacional de Desenvolvimento Científico e Tecnológico (CNPq) and Coordenação de Aperfeiçoamento de Pessoal de Nível Superior (CAPES) for financial support.

REFERENCES

[1] C. A. Britez and C. N. Costa, *Ações do Fogo nas Estruturas de Concreto*. São Paulo: Concreto Ciência e Tecnologia, 2011.

[2] G. C. Isaia, *A Evolução do Concreto Estrutural*. São Paulo: Concreto Ciência e Tecnologia, 2011.

[3] V. P. Silva, *Projeto de Estruturas de Concreto em Situação de Incêndio*, 2. ed. São Paulo: Blucher, 2016.

[4] A. M. Neville, *Propriedades do Concreto*, 5. ed. Porto Alegre: Bookman, 2016.

[5] P. Mehta, P. Kuma, and P. J. M. Monteiro, *Concreto: Microestrutura, Propriedades e Materiais*, 3. ed. São Paulo: IBRACON, 2008.

[6] Q. Zhang, G. Ye, and E. Koenders, "Investigation of the structure of heated Portland cement paste by using various techniques," *Constr. Build. Mater.*, vol. 38, pp. 1040–1050, Nov 2013, http://dx.doi.org/10.1016/j.conbuildmat.2012.09.071.

[7] V. Kodur, "Properties of concrete at elevated temperatures," *Int. Sch. Res. Notices*, vol. 2014, pp. 1–15, Mar 2014, http://dx.doi.org/10.1155/2014/468510.

[8] V. Paulon, A.P. Kirchheim, *Nanoestrutura e Microestrutura do Concreto Endurecido*, São Paulo: Concreto Ciência e Tecnologia, 2011.

[9] G. Robert, H. Colina, and G. Debicki, "*A durabilidade do concreto mediante ao fogo*," in: *Durabilidade do Concreto: Bases Científicas para a Formulação de Concretos Duráveis de Acordo com o Ambiente*, J. P. Ollivier and A. Vichot, Eds. São Paulo: IBRACON, 2014.

[10] A. H. Acka and N. Özyurt, "Post-fire mechanical behavior and recovery of structural reinforced concrete beams," *Constr. Build. Mater.*, vol. 253, pp. 1–10, Apr 2020, http://dx.doi.org/10.1016/j.conbuildmat.2020.119188.

[11] A. F. Battagin and A. L. Z. P. Silveira, "Estudo da microestrutura do concreto em situação e incêndio: um termômetro da temperatura alcançada," *Concreto Construcoes*, vol. 89, pp. 44–48, Jan 2018.

[12] E. Annerel and L. Taerwe, "Revealing the temperature history in concrete after fire exposure by microscopic analysis," *Cement Concr. Res.*, vol. 39, pp. 1239–1249, Aug 2009, http://dx.doi.org/10.1016/j.cemconres.2009.08.017.

[13] M. Vetter et al., "The use of Raman spectroscopy to monitor phase changes in concrete following high temperature exposure," *Constr. Build. Mater.*, vol. 204, pp. 450–457, Feb 2019, http://dx.doi.org/10.1016/j.conbuildmat.2019.01.165.

[14] C. S. Pilai et al., "Evaluation of microstructural and microchemical aspects of high density concrete exposed to sustained elevated temperature," *Constr. Build. Mater.*, vol. 126, pp. 453–465, Sep 2016, http://dx.doi.org/10.1016/j.conbuildmat.2016.09.053.

[15] T. Kerr, M. Kerr, and J. G. Rodriguez, "Evaluating residual compressive strength of post-fire concrete using Raman Spectroscopy," *Forensic Sci. Int.*, vol. 325, pp. 110874, Jun 2021, http://dx.doi.org/10.1016/j.forsciint.2021.110874.

[16] R. Ongah, P. Mendis, and J. Sanjayan, “Fire performance of high strength reinforced concrete walls”, in *ACMSM*, Y. C. Loo et al., Eds., pp. 199-204, Lisse: Netherland: A A Balkema, 2002.

[17] D. L. Peña, V. Albero, C. Ibáñes, and A. Hospitaler, “Sectional model for the fire evaluation of reinforced concrete columns subjected to biaxial bending,” *Eng. Struct.*, vol. 247, Nov 2021, http://dx.doi.org/10.1016/j.engstruct.2021.113094.

[18] R. C. S. Souza, M. Andreine, S. L. Mendola, J. Zefub, and C. Knaust, “Probabilistic thermo-mechanical finite element analysis for the fire resistance of reinforced concrete structures,” *Fire Saf. J.*, vol. 114, pp. 22–33, Mar 2019, http://dx.doi.org/10.1016/j.firesaf.2018.12.005.

[19] Associação Brasileira de Normas Técnicas, *Componentes Construtivos Estruturais - Determinação da Resistência ao Fogo*, NBR 5628, 2001.

[20] K. L. Mata et al., “Análise das temperaturas de um compartimento durante treinamentos de combate a incêndio,” *Ambient. Constr.*, vol. 20, pp. 245–260, 2020, http://dx.doi.org/10.1590/s1678-86212020000200398.

[21] A. L. Seito, *A Segurança Contra Incêndio no Brasil*. São Paulo: Projeto, 2008.

[22] C. A. Britez, “Avaliação de pilares de concreto armado colorido de alta resistência, submetidos a elevadas temperaturas”, M.S. thesis, São Paulo, Brasil, Departamento de Engenharia Civil, Escola Politécnica da USP, 2011. [Online] Avaliable: https://www.teses.usp.br/teses/disponiveis/3/3146/tde-31052011-170216/pt-br.php.

[23] B. Fernandes et al., “Microstructure of concrete subjected to elevated temperatures: physico-themical changes and analysis techniques,” *IBRACON Struct. Mater. J.*, vol. 10, no. 4, pp. 838–863, Sept 2017, http://dx.doi.org/10.1590/S1983-41952017000400004.

[24] J. S. K. Rama and B. S. Grewal, “Evaluation of efficiency of non-destructive testing methods for determining the strength of concrete damaged by fire,” *Adv. Struct. Eng.*, vol. 3, pp. 2567–2578, Jan 2015, http://dx.doi.org/10.1007/978-81-322-2187-6_198.

[25] H. S. Alcaíno, C. Manga-Verdugo, and L. López, “Experimental fast-assessment of post-fire residual strength of reinforced concrete frame buildings based on non-destructive tests,” *Constr. Build. Mater.*, vol. 234, pp. 117371, Nov 2019, http://dx.doi.org/10.1016/j.conbuildmat.2019.117371.

[26] E. Hwang, G. Kim, G. Choe, M. Yoon, N. Gucunski, and J. Nam, “Evaluation of concrete degradation depending on heating conditions by ultrasonic pulse velocity,” *Constr. Build. Mater.*, vol. 171, pp. 511–520, 2018, http://dx.doi.org/10.1016/j.conbuildmat.2018.03.178.

[27] Associação Brasileira de Normas Técnicas, *Projeto de Estruturas de Concreto em Situação de Incêndio*, NBR 15200, 2012.

[28] Y. S. Kim, Y. Ohmiya, M. Kanematsu, and G. Y. Kim, “Effect of aggregate on residual mechanical properties of heated ultrahigh-strength concrete,” *Mater. Struct.*, vol. 49, no. 9, pp. 3847–3859, Aug 2016, http://dx.doi.org/10.1617/s11527-015-0758-4.

[29] European Committee for Standardization, *Design of Concrete Structures – part 1.2: General Rules – Structural Fire Design,* Eurocode 2, 2004.

[30] Associação Brasileira de Normas Técnicas, *Concreto para Fins Estruturais - Classificação pela Massa Específica, por Grupos de Resistência e Consistência,* NBR 8953, 2015.

[31] Associação Brasileira de Normas Técnicas, *Concreto - Procedimento para Moldagem e Cura de Corpos de Prova,* NBR 5738, 2016.

[32] RILEM Technical Committee 200-HTC, “Recommendation of RILEM TC 200-HTC: mechanical concrete properties at high temperatures—modelling and applications,” *Mater. Struct.*, vol. 40, pp. 855–864, 2007, https://doi.org/10.1617/s11527-007-9286-1.

[33] RILEM Technical Committee 200-HTC, “Recommendation of RILEM TC 200-HTC: mechanical concrete properties at high temperatures—modelling and applications,” *Mater. Struct.*, vol. 40, pp. 841–853, 2007, https://doi.org/10.1617/s11527-007-9285-2.

[34] Associação Brasileira de Normas Técnicas, *Concreto - Ensaio de compressão de corpos de prova cilíndricos,* NBR 5739, 2018.

[35] D. Breysse et al., “Recommendation of RILEM TC249-ISC on non destructive in situ strength assessment of concrete,” *Mater. Struct.*, vol. 52, pp. 01–21, 2019, https://doi.org/10.1617/s11527-019-1369-2.

[36] A. Nonat “A hidratação dos cimentos”, in: *Durabilidade do Concreto-Bases Científicas para Formulação de Concretos Duráveis de Acordo com o Ambiente*, J. P. Olivier et al., Eds. São Paulo, Brasil: IBRACON, 2014, ch. 2.

[37] T. Schmida and P. Dariz, “Shedding light onto the spectra of lime: raman and luminescence bands of CaO, $Ca(OH)_2$ and $CaCO_3$,” *J. Raman Spectrosc.*, vol. 46, pp. 141–146, Dec 2014.

[38] S. Pesková, V. Machovic, and P. Procházka, “Raman spectroscopy structural study of fired concrete,” *J. Ceram. Silikaty*, vol. 55, pp. 410–417, Oct 2011.

[39] R. J. Kirkpartick et al., “Raman spectroscopy of C-S-H, tobermorite, and jennite,” *Adv. Cement Base. Mater.*, vol. 5, pp. 93–99, May 1997, http://dx.doi.org/10.1016/S1065-7355(97)00001-1.

[40] S. S. Potgieter-Vermaak, J. H. Potgieter, M. Belleil, F. DeWeerdt, and R. Van Grieken, “The application of Raman spectrometry to the investigation of cement: Part II: a micro-Raman study of OPC, slag and fly ash,” *Cement Concr. Res.*, vol. 36, pp. 663–670, Sep 2005, http://dx.doi.org/10.1016/j.cemconres.2005.09.010.

[41] N. Garg, “Raman spectroscopy for characterizing and determining the pozzolanic reactivity of fly ashes”, M.S. thesis, Iowa State University, Ames, Iowa, USA, 2012. https://doi.org/10.31274/etd-180810-1904

[42] G. Renaudin, R. Segni, D. Mentel, J. M. Nedelec, F. Leroux, and C. Taviot-Gueho, "A Raman study of the sulfated cement hydrates: ettringite and monosulfoaluminate," *J. Adv. Concr. Technol.*, vol. 5, pp. 299–312, Nov 2007, http://dx.doi.org/10.3151/jact.5.299.

[43] I. Hager, "Behavior of cement concrete at high temperature," *Bull. Pol. Acad. Sci. Tech. Sci.*, vol. 61, no. 1, pp. 1–10, 2013, http://dx.doi.org/10.2478/bpasts-2013-0013.

Author contributions: EWFS: conceptualization, methodology, bibliographic research, data analysis, supervision, drafting and writing; DAN: conceptualization, formal analysis, methodology and writing; CODM and EMS: data analysis, writing and formal analysis; MDSM: data analysis, methodology, writing and formal analysis; CPS: methodology, formal analysis and writing; SG: supervision, drafting, writing and formal analysis.

Editors: Lia Pimentel, Guilherme Aris Parsekian.